Note

Comparison of Different Random Vibrations for a Packaging Test

Daichi NAKAI[*,**] and Katsuhiko SAITO[*]

A random vibration test is important for confirming the safety of packaging on a truck bed during transportation. There are differences between the random vibration generated by the traditional method and the real vibration measured on a truck bed. Multiple studies have been performed to improve the generation of vibrations during testing. These methods are broadly divided into two categories: non-stationary and stationary. Since advantages and exist for both methods, they need to be compared under the same conditions. To date, there are no studies that compare stationary and non-stationary methods. Herein, seven different methods (both stationary and non-stationary methods) are used to generate vibrations. The generated vibrations are evaluated by statistics, the moving root mean square, and the kurtosis response spectrum. In terms of the kurtosis response spectrum, the kurtosis response method (a stationary method) is the closest to the real vibration, especially when the damping factor is low.

Keywords: Transportation, Vibration test, Response Spectrum, Kurtosis

1. Introduction

1.1 Methods for generating non-stationary random vibration

Random vibration laboratory testing is important for confirming the safety of packaging and goods being transported on a truck bed. A widely used traditional method for this testing is to utilize Gaussian vibrations based on the power spectral density (PSD) of the acceleration according to the standard JIS Z0232:2020 [1]. However, it has been pointed out that there are differences between the real vibration on the truck bed and the vibration generated by the traditional method. Multiple studies exist to improve the vibrations generated during testing. These methods are broadly divided into two methods: non-stationary and stationary [2].

The non-stationary methods combine the Gaussian vibrations with different intensities [2–4]. The advantage of the non-stationary methods is that they successfully reproduce the fluctuation of vibration intensity on a truck bed with a time range of more than a few seconds [2]. Conversely, a disadvantage of non-stationary methods is that statistical values (such as the acceleration kurtosis K_a) tend to deviate from the real vibration.

The stationary methods distort the vibration so that the statistical values (such as K_a) are close to those of a real vibration. Winterstein proposed a method by using a Hermite polynomial [5]. Hosoyama et al. proposed a method by controlling phase differentials [6]. The disadvantage of the stationary methods, compared with the non-stationary methods, is that the fluctuation of the vibration intensity on a truck bed is difficult to achieve [2].

In previous studies, the authors of this study proposed a method to generate vibrations controlling not only

* Transport Packaging Laboratory, Kobe University, 5-1-1, Fukaeminami, Higashinada, Kobe 658-0022, Japan
** Sankyu Inc. 16-1 Tsukiji, Yahatanishi, Kitakyushu, 806-0001, Japan
Corresponding author: Daichi Nakai. Tel: 093-645-7262 E-mail: d.nakai@sankyu.co.jp

the K_a but also the velocity [7]. This is a kind of stationary method that uses a phase differential. The effectiveness of the proposed method was verified by the kurtosis response spectrum. The kurtosis response spectrum is explained in section 1.2. The authors also proposed a method controlling the kurtosis response spectrum by varying the value of the phase differential at each frequency (kurtosis response method) [8].

1.2 Comparison of different random vibrations

A quantitative comparison study under the same conditions is needed to verify the effectiveness of the improvements since the proposed methods all have their own advantages and disadvantages. Zhou et al. generated vibrations by four methods and compared their statistics with those of the real vibration [9]. However, this study does not consider the damage to the products. Griffiths et al. proposed a device for estimating the scuffing damage and compared several generated vibrations with a real vibration [10]. This study focuses on the scuffing damage and does not consider the natural frequency of the product. In addition, both studies only focused on the non-stationary method and did not evaluate the stationary method.

Hosoyama et al. proposed the kurtosis response spectrum as a characteristic of vibration for packaging [11]. The kurtosis response spectrum assumes the single-degree-of-freedom (SDOF) model and calculates the kurtosis of the outputs at various natural frequencies. The kurtosis response spectrum has the advantage that the effects of a vibration can be evaluated for each natural frequency. It was showed that the kurtosis response spectrum varies with the natural frequency of the SDOF model when the input vibration is the real vibration measured on the truck bed [8), 11]. Hence it is assumed that a random vibration with a kurtosis response spectrum that is the same as that of the real vibration is similar to the real vibration.

In our previous study, the validation using the kurtosis response spectrum is a comparison between three methods [8]. However, the traditional method (JIS), the non-statinary methods and the Hermite polynomial method were not evaluated. Therefore, the aim of this study is to quantitatively compare the vibrations generated by various methods with the real vibration. Table 1 shows the vibrations this study utilizes. The vibrations of (a), (f), (g), and (h) in Table 1 are the same as those evaluated in the previous study [8].

Table 1 Evaluated vibrations in this study.

	Type
(a)Real Vibration [8]	
(b)Traditional (JIS) [1]	
(c)RMS split [3]	Non-Stationary
(d)Gaussian decomposition [4]	Non-Stationary
(e)Hermite polynomial [5]	Stationary
(f)Kurtosis response (T_d=16 s) [8]	Stationary
(g)Phase differential (T_d= 2 s) [6), 8]	Stationary
(h)Phase differential (T_d= 16 s) [7),8]	Stationary

2. Experiment [8]

The vertical vibration data for the truck bed were used as a target [Table 1(a)]. Fig. 1 shows the truck used in the experiment. An accelerometer (DER-1000, Shinyei Technology Co., Ltd.) was fixed to the truck bed. The truck was driven on the highway for 1,200 s (low-pass filter, 100 Hz).

Fig. 1 Truck used for testing [8].

3. Calculation

3. 1 Traditional method

The traditional method for generating random vibration is expressed by equation (1), as follows:

$$a(t) = \sum_{k=1}^{L} A_{\mathrm{k}} \cos(2\pi \Delta f t + \phi_{\mathrm{k}}), \quad (1)$$

where L, A_{k}, Δf, and ϕ_{k} are the number of frequency components, the amplitude, the frequency resolution, and the k_{th} phase angle, respectively. The term A_{k} is expressed by equation (2), as follows:

$$A_{\mathrm{k}} = \sqrt{2\Delta f P(k\Delta f)}, \quad (2)$$

where $P(k\Delta f)$ is the PSD. In traditional random vibration tests, ϕ_{k} denotes random numbers ranging from 0 to 2π.

3. 2 Root mean square split method

To decompose a real vibration into a low- and high-amplitude event, the root mean square (RMS) is sometimes used as a criterion. The real vibration was divided into 1-s segments, and the RMS was calculated. The real vibration was then divided into the lower 70% and upper 30% of the RMS value [3].

3. 3 Gaussian decomposition method

Rouillard proposed a method for generating random vibration with a non-Gaussian probability density distribution by combining Gaussian vibrations with different intensities [4]. Letting the probability density distribution of the real vibration be $p_1(a)$, it can be expressed by equation (3):

$$p_1(a) = \sum_{\mathrm{i}=1}^{n} p_{\mathrm{Gi}}(a) = \sum_{\mathrm{i}=1}^{n} \frac{D_{\mathrm{i}}}{\sqrt{2\pi}\sigma_{\mathrm{i}}} \exp\left(-\frac{a^2}{2{\sigma_{\mathrm{i}}}^2}\right), (3)$$

where $p_{\mathrm{Gi}}(a)$, σ_{i}, and D_{i} are the probability density of the i-th Gaussian, the standard deviation of the i-th Gaussian, and the vibration dose of the i-th Gaussian, respectively. Taking the logarithm of both sides of equation (3), equation (3) is transformed into equation (4), as follows:

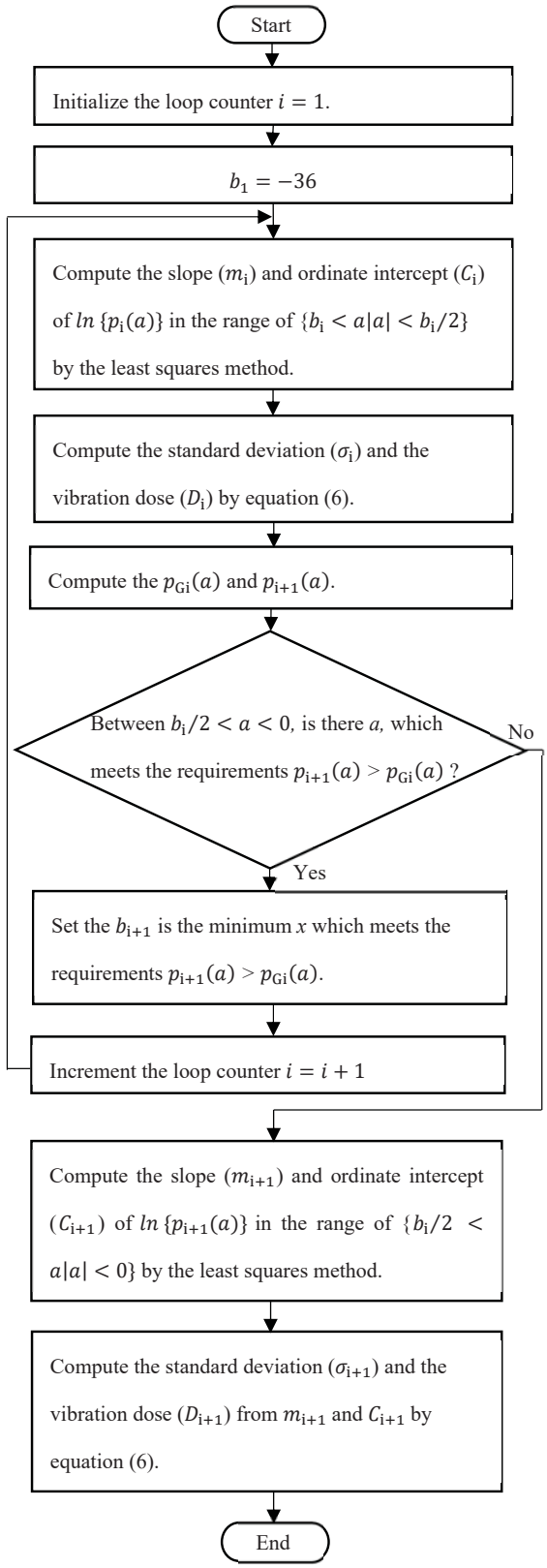

Fig. 2 Flowchart of the method used to decompose the real vibration into a Gaussian sequence.

$$ln\{p_1(a)\} = \sum_{i=1}^{n}\left\{ln\left(\frac{D_i}{\sqrt{2\pi}\sigma_i}\right) - \frac{1}{2{\sigma_i}^2}a|a|\right\}. \quad (4)$$

Plotting $a|a|$ on the horizontal axis and $ln\{p_i(a)\}$ on the vertical axis, the i-th Gaussian distribution ($a < 0$) has the slope $1/2{\sigma_i}^2$ and the intercept $ln\{D_i/\sqrt{2\pi}\sigma_i\}$. If the slope m_i and the intercept C_i are obtained by linearly approximating the probability density distribution in an interval, m_i and C_i are expressed by equation (5):

$$m_i = \frac{1}{2{\sigma_i}^2}, C_i = ln\left\{\frac{D_i}{\sqrt{2\pi}\sigma_i}\right\}. \quad (5)$$

Calculating equation (5), σ_i and D_i are expressed by equation (6), as follows:

$$\sigma_i = \frac{1}{\sqrt{2m_i}},\ D_i = \sqrt{\frac{\pi}{m_i}}\exp(C_i). \quad (6)$$

The term $p_{i+1}(a)$ was calculated by separating the i-th Gaussian distribution $p_{Gi}(a)$ from $p_i(a)$, as is expressed in equation (7):

$$p_{i+1}(a) = p_i(a) - p_{Gi}(a). \quad (7)$$

Figure 2 shows the flowchart of the method used to decompose the real vibration into the Gaussian sequence utilized in this study. The original proposed method showed the way to decompose it automatically. However, in this study, the flowchart, the range of approximation $\{b_i < a|a| < b_i/2\}$, and its initial value b_1 were manually adjusted so the real vibration could be successfully divided into four Gaussian distributions.

3. 4 Hermite polynomial

Winterstein proposed a method of generating vibration with an arbitrary K_a and an acceleration skewness V_a by distorting a Gaussian vibration using a Hermite polynomial [5]. A non-Gaussian acceleration $\hat{a}$ is calculated from a Gaussian acceleration a as expressed in equation (8):

$$\frac{\hat{a} - \mu_a}{\sigma_a} = \gamma\{a - h_3(a^2 - 1) + h_4(a^3 - 3a)\}. \quad (8)$$

The terms $\mu_a, \sigma_a, h_3, h_4$, and γ are the mean value of Gaussian acceleration, the standard deviation of Gaussian acceleration, the third Hermite moment, the fourth Hermite moment, and the scaling factor, respectively. The terms h_3, h_4, and γ are expressed by equations (9), (10), and (11), respectively:

$$h_3 = \frac{V_a}{4 + 2\sqrt{1 + 1.5(K_a - 3)}}, \quad (9)$$

$$h_4 = \frac{\sqrt{1 + 1.5(K_a - 3)} - 1}{18}, \quad (10)$$

$$\gamma = \sqrt{1 + 2{h_3}^2 + 6.5{h_4}^2}. \quad (11)$$

3.5 Phase differential method and kurtosis response method

In the traditional method, ϕ_{k} are independent of each other, but in the phase differential method, they are related by neighboring frequencies, as is expressed by equation (12):

$$\phi_{\mathrm{k}} - \phi_{\mathrm{k}-1} = 2\pi\Delta f t_{\mathrm{gr}}(k\Delta f), \quad (12)$$

where $t_{\mathrm{gr}}(k\Delta f)$ is a group-delay time. The term $t_{\mathrm{gr}}(k\Delta f)$ is taken as a random number with an average value m and a standard deviation σ [6]. The term σ is related to the sharpness of the envelope curve and the acceleration kurtosis K_{a}. Furthermore, Δf has an effect on the envelope curve and is related to the velocity kurtosis K_{v} and the period $T_{\mathrm{d}}(= 1/\Delta f)$, during which the maximum acceleration occurs [7]. The term T_{d} is set to 2 and 16 s to evaluate the vibrations with the same kurtosis of acceleration and different kurtosis of velocity.

The kurtosis response method controls the shape of the kurtosis response spectrum by varying the standard deviation σ for each of the corresponding frequencies in equation (12) [8].

3. 6 Kurtosis response spectrum analysis

In the original kurtosis response spectrum, the absolute acceleration response was used [11]. In this study, the relative displacement response was used because it is proportional to the strain of the product [8]. An SDOF system is expressed by equation (13), as follows:

$$m\left(\frac{d^2x(t)}{dt^2} + a(t)\right) + c\frac{dx(t)}{dt} + kx(t) = 0, \quad (13)$$

where t, m, c, k, $a(t)$, and $x(t)$ are the time, the mass, the viscosity coefficient, the spring constant, the input acceleration on the truck bed or vibration table, and the relative displacement between the mass and the truck bed, respectively. This equation was solved for $x(t)$ using the impulse response. In this system, the natural angular frequency ω_{n} equals $\sqrt{k/m}$ and the natural frequency f_{n} is $\omega_{\mathrm{n}}/2\pi$. The acceleration applied inside the SDOF structure $a_{\mathrm{i}}(t)$ is proportional to the relative displacement $x(t)$:

$$a_{\mathrm{i}}(t) = \frac{k}{m}x(t) = 4\pi^2 f_{\mathrm{n}}^2 x(t). \quad (14)$$

Here, f_{n} is from 1 to 100 Hz at intervals of 1 Hz. The damping factor $[\zeta(= c/2m\omega_{\mathrm{n}})]$ is changed from 0.04 to 0.24. The kurtosis of $a_{\mathrm{i}}(t)$ calculated for each natural frequency f_{n} (by fixing ζ) is the kurtosis response spectrum $K_{\zeta}(f)$.

3.7 Comprehensive evaluation of the kurtosis response spectrum

The differences between the kurtosis response spectra of the real vibration and the generated vibration were comprehensively evaluated by mean absolute error (MAE). The MAE is expressed by equation (15), as follows:

$$MAE = \frac{1}{100}\sum_{f=1}^{100}\left|K_{\zeta}(f) - K_{\zeta\_\mathrm{real}}(f)\right|, \quad (15)$$

where $K_{\zeta\_\mathrm{real}}(f)$ is the kurtosis response spectrum of the real vibration.

4. Results and Discussion

4. 1 Gaussian decomposition method

Table 2 shows the parameter and the results of the Gaussian decomposition method. Since the probability density distribution was approximated in order from the outer side, the smaller the value of i, the larger the value of σ_i. The sum of the vibration dose D_i equals to 1. The D_i multiplied by the overall vibration duration is the duration of the i-th Gaussian vibration.

Figure 3 shows the Gaussian decomposition on a log scale. When plotting $a|a|$ on the horizontal axis and $ln\{p_i(a)\}$ on the vertical axis (as is shown in Fig. 3), the probability density of the Gaussian distribution is a linear line. Each Gaussian distribution is well approximated per the approximation range in Table 2.

Table 2 The parameter and the results of the Gaussian decomposition.

	D_i	σ_i (m/s$_2$)	Approximation range
P_{g1}(a)	0.016	2.327	$-36 < a\|a\| < -18$
P_{g2}(a)	0.273	1.165	$-12.43 < a\|a\| < -6.21$
P_{g3}(a)	0.595	0.557	$-1.16 < a\|a\| < -0.58$
P_{g4}(a)	0.116	0.273	$-0.58 < a\|a\| < 0$
Sum	1.000		

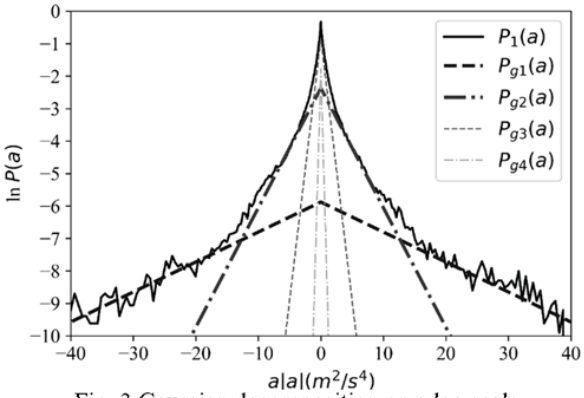

Fig. 3 Gaussian decomposition on a log scale.

4.2 Comparison of each vibration

Figure 4 shows the time series accelerations evaluated in this study. Fig. 4 (a), (f), (g), and (h) have already been reported in the previous study [8]. All generated vibrations are set to 1,200 s because the real vibration was 1,200 s. Fig. 4 (b) demonstrates the time series acceleration generated by the traditional method. Compared with the real vibration [Fig. 4 (a)], the traditional method was stationary and did not include shocking events. Fig. 4 (c) shows the time series acceleration generated by the RMS split method. The first 70% (0–840 s) is considered a section where normal vibration occurs, and the last 30% (840–1,200 s) is a section where shocking vibration occurs. Fig. 4 (d) shows the vibration generated by the Gaussian decomposition method. The Gaussian decomposition method was split into four segments and these Gaussian segments were arranged in ascending order of the RMS value σ_i. Fig. 4 (e) demonstrates the time series acceleration generated by the Hermite polynomial method. Unlike in the non-stationary method shown in Fig. 4 (c) and (d), there were no segments in the Hermite polynomial method. Compared with those in the traditional method, there are high accelerations of 5 m/s^2 or more in Fig. 4 (e). Fig. 4 (f), (g), and (h) show, respectively, the vibration generated by the kurtosis response method and the phase differential method (T_d = 2, 16 s). In Fig. 4 (f) and (h), the vibration repeated in strength and weakness regularly for a period of 16 s. In Fig. 4 (g), a period is 2 s.

Figure 5 demonstrates the time series velocity integrated from the time series acceleration with a low-cut filter (0.5 Hz) [12]. Fig. 5 (a), (f), (g), and (h) have already been reported in the previous study [8]. The maximum velocity of the real vibration was

over 0.6 m/s, the maximum velocities in Fig. 5 (b) and (g) were approximately 0.2 m/s, and the maximum velocities of the other vibrations were approximately 0.4 m/s.

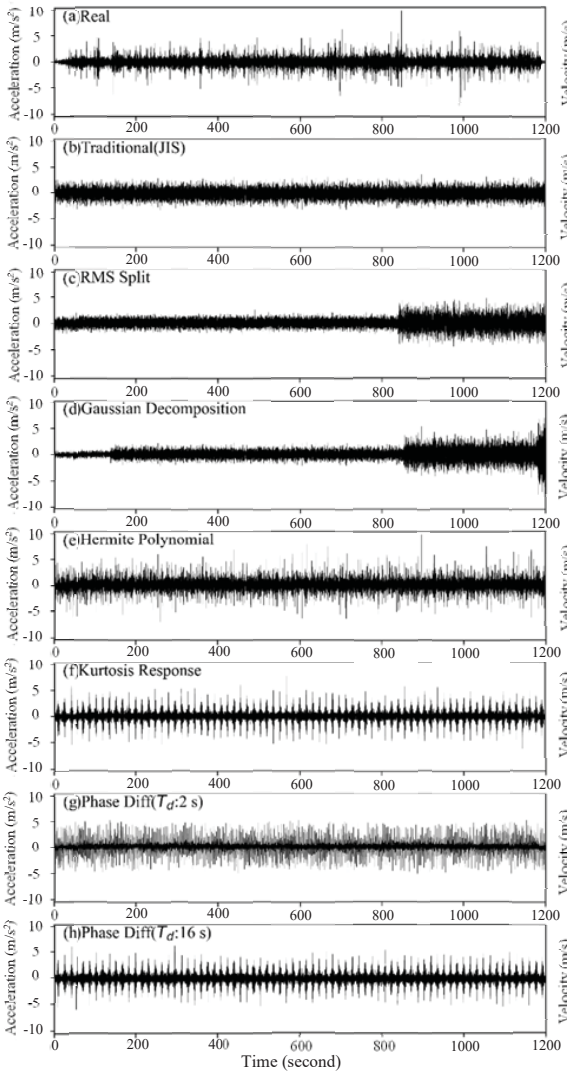

Fig. 4 Time series acceleration: (a) real, (b) traditional, (c) RMS split, (d) Gaussian decomposition, (e) Hermite polynomial, (f) kurtosis response, (g) phase difference (T_d: 2 s), and (h) phase difference (T_d: 16 s).

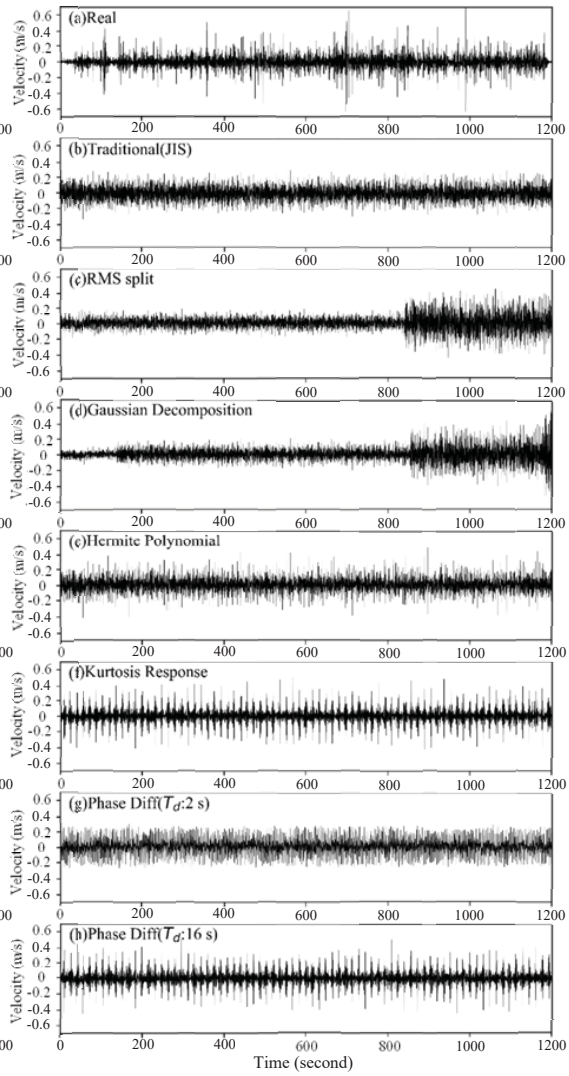

Fig. 5 Time series velocity: (a) real, (b) traditional, (c) RMS split, (d) Gaussian decomposition, (e) Hermite polynomial, (f) kurtosis response (g) phase difference (T_d: 2 s), and (h) phase difference (T_d: 16 s).

Table 3 Statistical values of real vibration and generated vibrations.

	Acceleration RMS (m/s^2)	Velocity RMS (m/s)	Acceleration Kurtosis	Velocity Kurtosis
(a) Real Vibration	0.796	0.0804	7.24	8.59
(b) Traditional (JIS)	0.796	0.0809	2.96	3.00
(c) RMS split	0.795	0.0820	5.15	5.68
(d) Gaussian decomposition	0.806	0.0820	6.96	6.80
(e) Hermite polynomial	0.804	0.0811	7.26	4.41
(f) Kurtosis response (T_d=16 s)	0.792	0.0800	7.20	6.59
(g) Phase differential (T_d= 2 s)	0.790	0.0832	7.24	3.65
(h) Phase differential (T_d= 16 s)	0.792	0.0798	7.18	6.41

Table 3 shows the statistical values of the real vibration and the generated vibrations. In Table 3, (a), (f), (g), and (h) have already been reported in the previous study [8]. There were no significant differences in the acceleration RMS and the velocity RMS between all vibrations. Both the K_a and the K_v of the traditional method were approximately 3 (Gaussian). Both the K_a and K_v of the non-stationary method [Table 3, (c) and (d)] were smaller than those of the real vibration. The K_a and K_v of the non-stationary method were close to each other. The K_a of the stationary methods [Table 3, (d)–(g)] were close to that of the real vibration because the stationary method can generate vibrations with an arbitrary K_a. In spite of similar K_a values with the real vibration, the K_v of the Hermite polynomial and the phase differential method (T_d = 2 s), both of which were smaller than its K_a, were much smaller than that of the real vibration. The K_v of the kurtosis response and the phase differential (T_d= 16 s) method were closer to that of the real vibration and bigger than those of the Hermite polynomial method and the phase differential (T_d= 2 s) method.

Figure 6 shows the PSD of acceleration. Fig 6 (a), (f), (g), and (h) have been already reported in the previous study [8]. There were no significant differences between all vibrations.

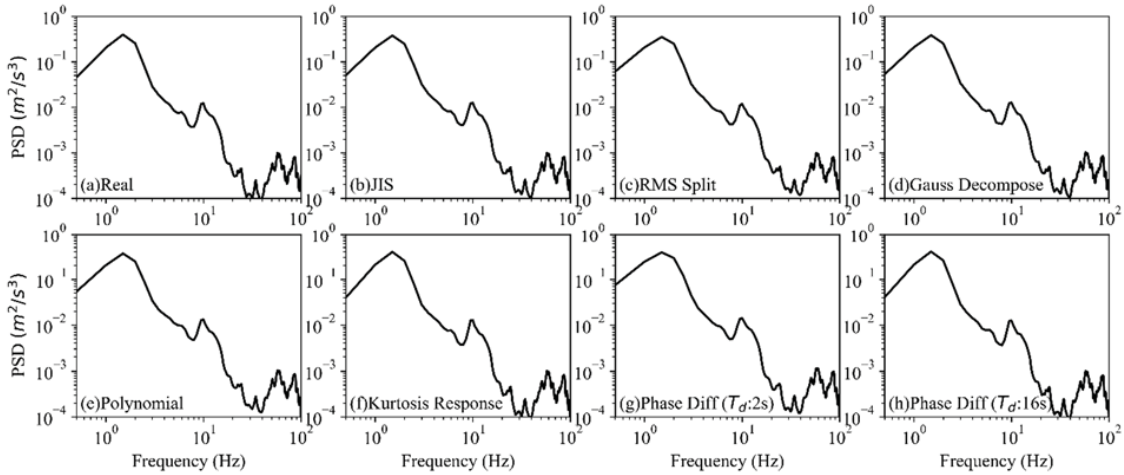

Fig. 6 Power spectral density: (a) real, (b) traditional, (c) RMS split, (d) Gaussian decomposition, (e) Hermite polynomial, (f) kurtosis response, (g) phase differential (T_d: 2 s), (h) phase differential (T_d: 16 s).

Figure 7 shows the probability density distribution of acceleration. Fig 7 (a), (f), (g), and (h) were already reported in the previous study [8]. The dotted lines in Fig. 7 show the Gaussian distributions (the standard deviations are shown in Table 3, and the mean is zero). Fig. 7 (b) shows that the probability density distribution of acceleration of the traditional method is close to the Gaussian distribution. The probability density distribution of the RMS split method [Fig 7 (c)] is wider than the Gau.ssian distribution but narrower than the real vibration. The shapes of the other probability density distributions [Fig. 7 (d)–(f) and (h)] are very similar to that of the real vibration, except for the shape of the phase differential method (T_d: 2 s) [Fig. 7 (g)].

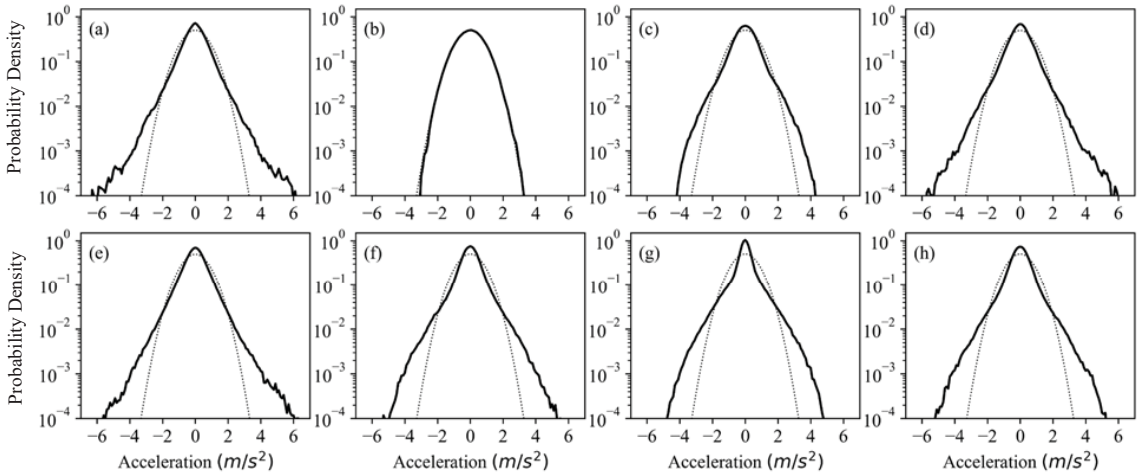

Fig. 7 Probability density distribution of acceleration: (a) real, (b) traditional, (c) RMS split, (d) Gaussian decomposition, (e) Hermite polynomial, (f) kurtosis response, (g) phase differential (T_d: 2 s), (h) phase differential (T_d: 16 s).

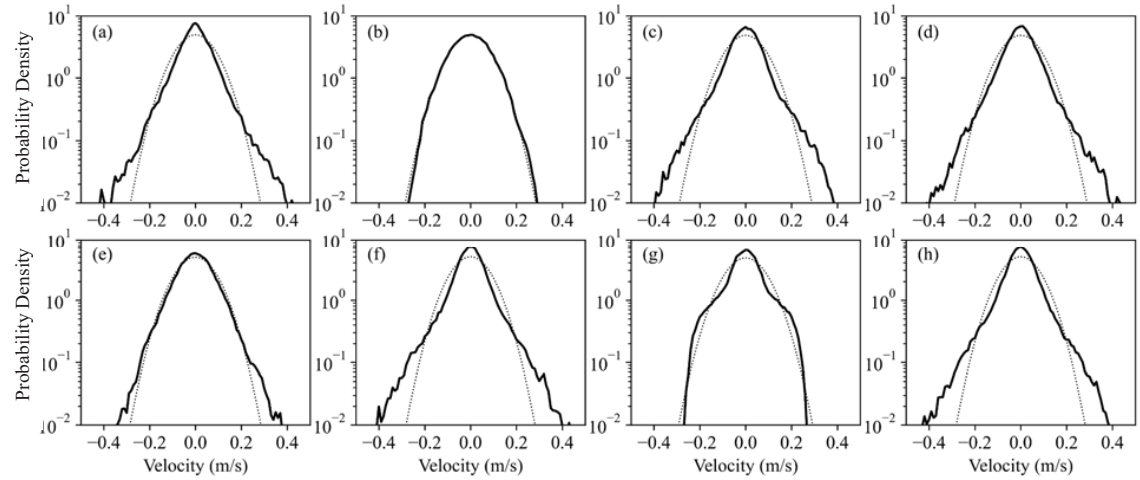

Fig. 8 Probability density distribution of velocity: (a) real, (b) traditional, (c) RMS Split, (d) Gaussian decomposition, (e) Hermite polynomial, (f) kurtosis response, (g) phase differential (T_d: 2 s), (h) phase differential (T_d: 16 s).

Figure 8 shows the probability density distribution of velocity. Fig. 8 (a), (f), (g), and (h) were already reported in the previous study [8]. The dotted lines in Fig. 8 show the Gaussian distributions (the standard deviations are shown in Table 3, and the mean is zero). The velocity of the traditional method was Gaussian, as is shown in Fig. 8 (b). The Hermite polynomial [Fig. 8 (e)] and the phase differential (T_d: 2 s) method [Fig. 8 (g)] had narrow probability densities of velocity compared with the real vibration, though the probability densities of acceleration were almost the same. The RMS split [Fig 8 (c)], the Gaussian decomposition [Fig. 8 (d)], the kurtosis response [Fig. 8 (f)], and the phase differential (T_d: 16 s) method [Fig. 8 (h)] had a probability density distribution similar to the real vibration.

Figure 9 shows the probability density distribution of the moving RMS (sometimes used as a criterion of vibration intensity variation) [2), 9)]. The window length of the moving RMS was 0.5 s in this study [9)]. As is shown in Fig. 9 (a), there were moving RMS greater than 2.0 m/s^2 in the real vibration. Unlike the real vibration, the moving RMS of the traditional method [Fig. 9 (b)], the Hermite polynomial [Fig 9 (e)], and the phase diff.erential (T_d: 2 s) method [Fig. 9 (g)] hardly exceeded 2.0 m/s^2. As is shown Fig. 9 (c), there were moving RMS greater than 2.0 m/s^2 in the RMS split method, but the shape of the probability density distribution was significantly different from the real vibration, especially below 1.0 m/s^2. The Gaussian decomposition [Fig. 9 (d)], the kurtosis response [Fig. 9 (f)], and the phase differential (T_d: 16 s) method [Fig. 9 (h)] had probability density distributions close to that of the real vibration.

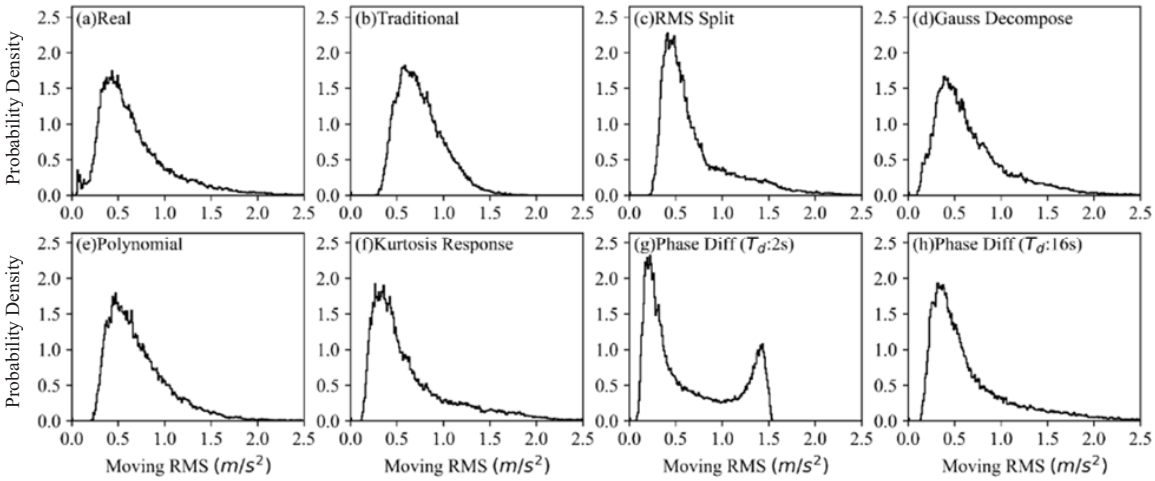

Fig. 9 Probability density distribution of the moving RMS (window length 0.5 s): (a) real, (b) traditional, (c) RMS split, (d) Gaussian decomposition, (e) Hermite polynomial, (f) kurtosis response, (g) phase differential (T_d: 2 s), (h) phase differential (T_d: 16 s).

Figure 10 (A), (B), (C), and (D) show the kurtosis response spectrum when the damping factor is 0.04, 0.08, 0.16, and 0.24, respectively. The right side of Fig. 10 (A), (B), and (C) were already reported in the previous study [8)]. Higher kurtosis response values resulted in greater damage to the product even if the PSDs were the same. The more the shape of the kurtosis response spectrum resembles that of the real vibration, the more the damage that occurs to the product during the vibration test are assumed to be similar to the real vibration.

Regardless of the natural frequency and the damping factor, the kurtosis response spectrum of the traditional method was approximately 3. This is equal to the Gaussian distribution. In addition, the shape of the kurtosis response spectrum became flatter as the damping factor increased, except in the traditional method.

In the stationary methods, such as the Hermite polynomial method and the phase differential (T_d: 2 s) method, the kurtosis response spectrum was smaller value at low frequencies (below 20 Hz) compared with the real vibration. As the kurtosis of velocity is low for both vibrations, it is assumed that the differences in response kurtosis between the real vibration and the low-frequency stationary vibrations were influenced by the difference in the kurtosis of velocity. Unlike those of the stationary methods, the kurtosis response spectra of the non-stationary methods (such as the RMS split method and the Gaussian decomposition method) were not small in

the low-frequency region. When the damping factor was 0.16 or 0.24, the kurtosis response spectra of the Gaussian decomposition method were particularly similar to those of the real vibration.

As was shown in the previous study, the kurtosis response spectrum of the kurtosis response method was close to that of the real vibration at a low damping factor (ζ = 0.04) [8]. The phase differential method (T_d: 16 s) with a higher kurtosis of velocity showed improvement in the low-frequency region and was close to the real vibration at a high damping factor (ζ = 0.16, 0.24).

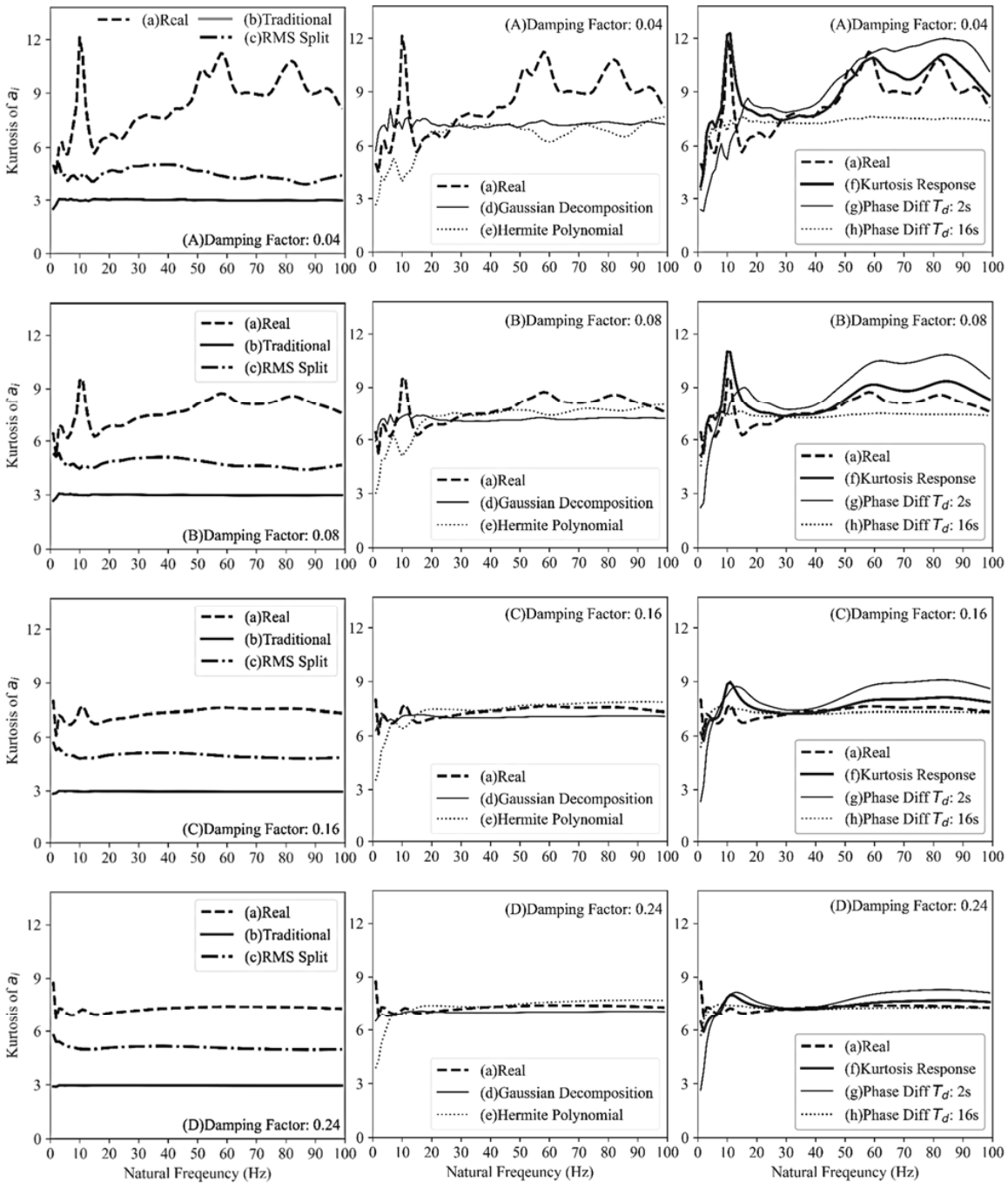

Fig. 10 Kurtosis response spectrum of $a_i(t)$: (A) ζ = 0.04, (B) ζ = 0.08, (C) ζ = 0.16, (D) ζ = 0.24.

The probability density distribution of the moving RMS and the kurtosis response spectra of the vibrations generated by the Gaussian decomposition method and the phase differential method (T_d: 16 s) had similar properties despite having completely different envelope shapes.

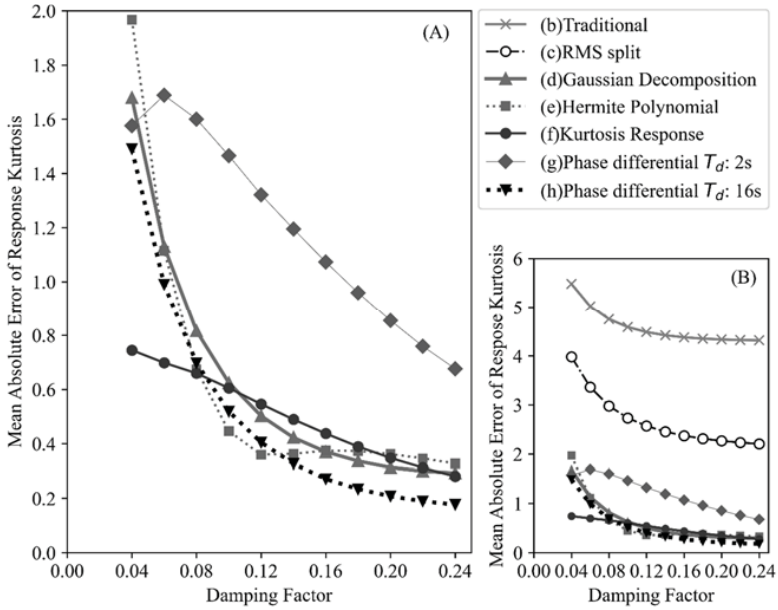

Fig. 11 Comparison of the generated vibrations using the mean absolute error of response kurtosis: (a) enlarged view; (b) overall view.

Figure 11 shows the MAE of the response kurtosis between the real and generated vibration. The smaller the MAE, the smaller the difference from the real vibration. As the damping factor increases, the MAE tends to decrease. This is due to the flattening of the shape of the response kurtosis spectrum as the damping factor increases.

The MAEs of the traditional method and the RMS split method were higher than that of the other vibrations. This is because the kurtosis response was smaller than those of the real vibration in all the natural frequencies and all the damping factors. The MAEs of the phase differential (T_d: 2 s) method were higher than those of (d), (e), (f), and (h) in Fig. 11. This is because in the low natural frequency region, the response kurtosis of the phase differential (T_d: 2 s) method was smaller than that of the real vibration, and in the high natural frequency region, the response kurtosis was higher than that of the real vibration. The MAE of the Hermite polynomial method was higher than that of the Gaussian decomposition method in the case of a low damping factor ($\zeta = 0.04$). This is due to the depression of the kurtosis response spectrum in the low natural frequency region.

In the case of a low damping factor ($\zeta \leq 0.08$), the smallest MAE was the vibration generated by the kurtosis response method. Even in the case of a high damping factor ($\zeta > 0.08$), the MAEs of the kurtosis response method were almost the same compared with those of the Gaussian decomposition method.

In the case of a high damping factor ($\zeta \geq 0.14$), the smallest MAE was the vibration generated by the phase differential method (T_d: 16 s). The MAE trends of the Gaussian decomposition method and the phase differential method (T_d: 16 s) were similar. However, the MAEs of the Gaussian decomposition method were slightly higher than that of the phase differential method (T_d: 16 s) for all damping factors. The K_a of the Gaussian decomposition method is assumed to be smaller than that of the real vibration. For example, the mean values of $K_{\xi = 0.24}$ were

7.28 for the real vibration, 7.00 for the Gaussian decomposition method, and 7.23 for the phase differential method (T_d: 16 s). These values were close to the K_a, as is shown in Table 3.

5. Conclusions

Seven vibrations generated by different methods (stationary and non-stationary) were compared with the real vibration. Compared with the stationary methods, the non-stationary methods (e.g., the Gaussian decomposition method) have the advantage that the response kurtosis spectrum does not decrease when the natural frequency of the product is small. Among the stationary methods, the method considering the K_v [the phase differential method (T_d: 16 s) and the kurtosis method] showed the same improvement in low natural frequency as the non-stationary methods. The mean absolute value of the response kurtosis was best with the kurtosis response method for low damping factors and best with the phase differential (T_d: 16 s) method for high damping factors.

The results of this study were based on a single highway transportation for 1,200 s. Therefore, further comparisons under various conditions are necessary.

References

1) JIS Z 0232:2020: Packaging-Complete, filled transport packages and unit loads- Method of vibration test.

2) V. Rouillard and M. A. Sek, Synthesizing nonstationary, non-Gaussian random vibrations, Packag. Technol. Sci., **23**(8), p423 (2010).

3) J. Singh, S. P. Singh and E. Joneson, Measurement and analysis of UK truck vibration for leaf spring and air ride suspensions and development of tests, Packag. Technol. Sci., **19**(6), p309 (2006).

4) V. Rouillard, On the non-Gaussian nature of random vehicle vibrations, World Congress on Engineering, London, UK, p1219 (2007).

5) S. R. Winterstein, Nonlinear vibration models for extremes and fatigue, Eng. Mech., **114**(10), p1772 (1988).

6) A. Hosoyama and T. Nakajima, The method of generating non-gaussian random vibration using kurtosis, J. Packag. Sci. Technol., Jpn, **20**(1), p27 (2011).

7) D. Nakai and K. Saito, A method for generating random vibration using acceleration kurtosis and velocity kurtosis. J. Appl. Packag. Res., **11**(2), p64 (2019).

8) D. Nakai and K. Saito, A method for generating random vibration considering kurtosis response spectrum, J. Packag. Sci. Technol., Jpn, **30**(4), p261 (2021).

9) H. Zhou and Z-W. Wang, Comparison study on simulation effect of improved simulation methods for packaging random vibration test, Packag. Technol. Sci., **32**(3), p119 (2019).

10) K. Griffith, D. Shires, W. White, P. S. Keogh and B. J. Hicks, Correlation Study Using Scuffing Damage to Investigate Improved Simulation Techniques for Packaging Vibration Testing, Packag. Technol. Sci., **26**(7), p373 (2013).

11) A. Hosoyama, K. Tsuda and S. Horiguchi, Development and validation of kurtosis response spectrum

analysis for antivibration packaging design taking into consideration kurtosis. Packag. Technol. Sci., **33**(2), p51 (2020).

12） D. Nakai and K. Saito, Estimation method of velocity change on truck bed, J. Packag. Sci. Technol., Jpn, **28**(1), p33 (2019).

(Received 19 August 2021)
(Accepted 12 November 2021)

包装試験におけるランダム振動の比較

中井 太地*, **、 斎藤勝彦*

輸送荷台での包装の安全性を確認するためにランダム振動試験は重要である。しかし従来の試験振動とトラックの荷台で測定される実際の振動には違いがあり、試験振動を改善する研究が行われている。これらの方法は非定常法と定常法に分けられるが、利点と欠点があり同条件で比較する必要がある。しかし我々の知る限り，非定常法と定常法を比較した研究は存在しない。本研究では非定常法と定常法を含む 7 つの方法を用いて振動を生成した。生成振動は、統計値、移動二乗平均平方根、尖度応答スペクトルを用いて実輸送と比較した。尖度応答スペクトルの観点から、定常法の一種の尖度応答法が、特に低減衰定数のとき実輸送と乖離が少なかった。

キーワード: 輸送、振動試験、尖度、応答スペクトル